Alteration of Payload in Extracellular Vesicles by Crosstalk With Mesenchymal Stem Cells From Different Origin

Dong Jun Park
  Yonsei University Wonju Medical College: Yonsei University Wonju College of Medicine

Jeong-Eun Park
  Yonsei University Wonju Medical College: Yonsei University Wonju College of Medicine

Tae Hoon Kong
  Yonsei University Wonju Medical College: Yonsei University Wonju College of Medicine

YoungJoon Seo (✉ okas2000@hanmail.net)
  Yonsei University - Wonju Campus   https://orcid.org/0000-0002-2839-4676

Abstract

Background

The application of extracellular vesicles (EVs) derived from mesenchymal stem cells (MSCs) requires customized materials to target disease or cell damage. We hypothesized that EVs exert different inflammatory effects on one recipient cell, although stem cells of different origins in humans have similar payloads.

Results

Here, the payload of EVs released by crosstalk between MSCs and human middle ear epithelial cells (HMEECs) extracted from adipose tissue, bone marrow and tonsils significantly increased the level of anti-inflammatory factors. EVs derived from the co-culture medium decreased *TNF-α, COX-2, IL-1β*, and *IL-6* levels to approximately zero within 3 h in HMEECs. Expression of miR-638 and amyloid-β A4 precursor protein-binding family A member 2 was analyzed using microarrays and gene ontology analysis, respectively.

Conclusions

In conclusion, stem cells of different origins have different payloads through crosstalk with recipient-specific cells. Inducing specific factors in EVs by co-culture with MSCs could be valuable in regenerative medicine.

Background

Otitis media (OM) is one of the most common diseases affecting children [1]. Although acute OM may resolve spontaneously, oral antibiotics and corticosteroids are ineffective in the long-term treatment of recurrent and chronic OM. Bacterial resistance to antibiotics has become an emerging problem in many parts of the world. Researchers have focused on understanding the pathophysiology of OM as a replacement for antibiotic treatment, including the role of inflammatory mediators and ion homeostasis molecules [2]. Restoration of fluid homeostasis function in the middle ear epithelium could be a target for future treatment, similar to the role of the upper respiratory ciliated mucosa. The middle ear mucosa is a pseudostratified, ciliated columnar epithelium through the eustachian tube that continues to the respiratory tract. Stem cell-derived exosomes control inflammatory signaling within the airway through intercellular communication, as demonstrated by the transfer of suppressor of cytokine signaling 1 from macrophage-derived exosomes to alveolar epithelial cells [3]. Human mesenchymal stem cell (hMSC)-derived extracellular vesicles (EVs) possess most of the anti-inflammatory and neuroprotective activities of MSCs in the respiratory epithelium [4, 5].

Therapeutics based on stem cell technology, including stem cell-derived EVs, have emerged in recent years and can treat what were otherwise considered incurable diseases in the field of cancer or cell regeneration [6]. Mesenchymal stem cells (MSCs) have been found to have different sources, such as the bone marrow, fat, urine, and tonsil; although they have the same phenotype, they are reported to have different internal payloads with various efficacies of treatments [5, 7]. It has been found that tumor-derived EVs play a key role in crosstalk between malignant and transformed cells and the immune system and that cancer cells suppress immune surveillance [8]. In addition, stem cell-derived EVs are involved in crosstalk with surrounding cells

during development and release their molecules to them [9, 10], and help the survival of surrounding cells through secretion via EVs of inflammatory, differentiation, and proliferation factors [4, 5].

EVs are a heterogeneous group of secreted membranous vesicles, including microvesicles, ectosomes, and exosomes [11]. They have become valuable biomarkers in liquid biopsies [12], and existing research has focused on their characterization in different cancer types [9]. When stem cells undergo autophagy through external stimulation, exocytosis is stimulated when intracellular multivesicular bodies (MVBs) increase, resulting in a large number of extracellular vesicles [13]. Furthermore, EVs are known to be released by a variety of human cells and are important mediators in the coordination of the immune response to maintain host homeostasis [5, 14]. Upon different stimulation, EVs carry different combinations of nucleic acids, proteins, and lipids to other cells [15] and have been reported to be associated with certain pathological conditions, particularly microbial infections and cancer [16]. It has also been reported that the amount of EVs released by external stimulation increases with time [13]. The ability to block the transfer of tumor-derived EVs containing oncogenic messages, such as EGFR, into recipient cells is a potential antitumor strategy. A study showed that incubation of EVs from a cell line with heparin blocked their transfer into recipient cells [17].

In this study, we evaluated the anti-inflammatory effect of EVs derived from hMSCs extracted from the adipose tissue, bone marrow, and tonsils. MSCs derived from these sources contain several factors related to cell proliferation and inflammation-reducing substances [18-20], but miRNA or cytokine expression and efficacy by crosstalk with new recipient cells may differ [14, 21]. Various studies have reported the relief of inflammation in skin tissues and infected organs in animal models [22]. The current focus of anti-inflammatory studies using MSC-derived EVs is to increase the payload of useful factors in EVs through discovery of factors through wound healing and mechanism research [23, 24]; there are reports that a calcium-dependent mechanism increases the release of EVs from the cells [25]. However, the important aspect of MSC research is to observe the change in payload inside the MSC and understands its role in disease [21]. In this study, we profiled the factors related to anti-inflammatory activity in EVs derived from MSCs extracted from different origins, when co-cultured with human middle ear epithelial cells (HMEECs), which can cause OM [26]. Interestingly, the expression level of molecule payload and anti-inflammatory efficiency were different in EVs from MSCs derived from adipose tissue, bone marrow, and tonsils co-cultured with HMEECs. Therefore, we propose a technology to discover new miRNA candidates by profiling it to prove inflammation relief according to the change of EV payload by crosstalk between MSCs and target cells is altered. In addition, the technique, involving the co-culture condition, offers a new direction for MSC-derived EV research to cure diseases or cancer; studies on the mechanism underlying the crosstalk between donor and recipient cells are also needed.

Materials And Methods

Extraction of mesenchymal stem cells (MSCs) derived from adipose tissue, bone marrow, and tonsils

The human adipose tissue, bone marrow, and tonsils were obtained from the iliac crest of patients who received transplantation treatment at the Wonju Severance Christian Hospital after obtaining their written consent (IRB number: CR320104). The extraction of adipose tissue-derived MSCs was performed as

described by Cho et al. [18]. Briefly, the tissue samples were washed twice with phosphate-buffered saline (PBS, D8537, Sigma-Aldrich, MA, USA) to remove blood cells and incubated with 200 IU/mL collagenase (Thermo Fisher Scientific, Carlsbad, CA, USA) for 45 min at 37°C. After incubation, the samples were centrifuged at $300 \times g$ for 7 min, the supernatant was discarded, and the remaining pellets were resuspended in MEM-alpha (Hyclone, Logan, UT, USA) with 10% fetal bovine serum (FBS) (Gibco, Grand Island, NY, USA) and antibiotics (anti-anti, Thermo Fisher Scientific, Carlsbad, CA, USA). The cells were transferred to a culture plate and incubated in a humidified atmosphere of 95% air and 5% CO_2 at 37°C.

To extract MSCs derived from the bone marrow, aspirates were collected into Vacutainers K2 EDTA (BD Biosciences, San Jose, CA, USA). The mononuclear cells were diluted 1:5 with PBS and separated by density gradient centrifugation at $435 \times g$ for 20 min at room temperature (RT, 25°C) using a Ficoll Hypaque (GE17-1440-02, Gibco, Grand Island, NY, USA) solution. The cell fractions were collected and cultured using MEM-alpha with 10% FBS and antibiotics at a seeding density of 5×10^3 cells per cm^2. The plate was maintained at 37 °C in a humidified atmosphere containing 5% CO_2. To exchange the medium, the plate was washed with PBS to remove the non-adherent cells, and the medium was replaced. Upon reaching 70% confluence, the cells were passaged to 1×10^6 cells/plate.

Tonsil-derived MSCs were extracted as described by Bacic et al. [27]. The tonsil tissue was gently washed with ethanol and cut with surgical scissors on a plate. After washing with PBS, the tissue mixture was added to Falcon tubes and incubated with PBS, 200 IU/mL collagenase, and 10 µg/mL DNase (EN0525, Thermo Fisher Scientific, Carlsbad, CA, USA) at 37°C in a water bath for 1 h. After filtering the suspension using a cell strainer, the monocytes were isolated from the supernatant using Ficoll Hypaque density gradient centrifugation. The cell fractions were collected and cultured using MEM-alpha with 10% FBS and antibiotics at a seeding density of 5×10^3 cells per cm^2.

Flow cytometric analysis

Flow cytometry was used to assess the immune profile of MSCs using the standard for MSCs, as described by the International Society for Cellular Therapy (ISCT) [28]. The cell surface markers were analyzed using a human MSC (hMSC) analysis kit (562245, BD Biosciences, San Jose, CA, USA). According to the manufacturer's instructions, the hMSC-positive cocktail (CD90 FITC, CD105 PerCP-Cy5.5, and CD73 APC) and PE hMSC negative cocktail (CD34, CD11b, CD19, CD45, and HLA-DR) were used as the positive and negative controls, respectively. The hMSC Positive Isotype Control Cocktail (mIgG1κ FITC, mIgG1 κ PerCP-Cy5.5, and mIgG1 κ APC) and PE hMSC Negative Isotype Control Cocktail in the kit (mIgG1 κ PE and mIgG2a κ PE) were also used as an isotype control for the analysis. The samples were analyzed through flow cytometry using a FACS Aria3 flow cytometer (Becton Dickinson, San Jose, CA, USA). The data were analyzed using the FACS Diva software.

Culture of human middle ear epithelial cells

HMEECs were provided by Dr. David J. Lim (House Ear Institutes, Los Angeles, CA, USA). The cells were immortalized with the E6/E7 genes of the human papillomavirus [29] and cultured in Dulbecco's modified

Eagle's medium (Lonza, MD, USA) and bronchial epithelial basal medium (Lonza, 1:1). The medium was changed every 3 days after washing with PBS. The cells were then humidified at 37°C with 5 % CO_2.

Isolation of extracellular vesicles

To obtain EVs, initial extraction was performed according to the MISEV guidelines as far as possible [30]. The cells were cultured in a serum-free environment for protein analysis and NTA analysis based on MSC-derived EVs. After centrifuging the cells and debris, the medium was collected and centrifuged at 2,000 × g for 30 min, and the total exosome isolation reagent (4478359, Invitrogen, Grand Island, USA) was used according to the manufacturer's instructions. To purify EVs from the fractions, we centrifuged the fraction at 10,000 × g for 1 h at 4°C on the next day and added 200 μL of PBS to the sunk pellets to dissolve them. The samples were centrifuged at 22,000 × g for 2 h at 4°C using a table microcentrifuge (5424R, Eppendorf, Germany) to obtain high-purity EVs.

Transwell study

Co-culture conditions employed in this study were reported by Lu et al. [31]. One million MSCs were seeded into a transwell insert with a 0.4-μm pore size (3401, Corning, NY, USA) consisting of a polycarbonate membrane. MSCs derived from adipose tissue, bone marrow, and tonsil were co-cultured with HMEECs in the inner well. In addition, HMEECs were seeded into the outer well. They were then carefully transferred and cultured in a 37°C incubator with 5% CO_2 in a humidified atmosphere prior to the appropriate LPS treatment or isolation of EVs from the media.

Cell viability assay

Cell viability was measured using a cell counting kit according to the manufacturer's instructions (CCK-300, Seoul, Korea). The cells were seeded at 1×10^3 cells per well in a 96-well plate. After exposure to 1, 5, 10, and 100 μg/mL LPS for different periods of time, CCK-8 solution was added to each well and the plates were incubated for 4 h at 37°C. Cell viability was also measured after HMEECs were co-cultured with MSCs for 24 h. The plate was mixed thoroughly using a shaker, and the optical density was measured at 450 nm using a microplate reader (Epoch, BioTek, VT, USA).

Real-time PCR

To evaluate the expression of the inflammatory markers, total RNA was isolated from HMEECs after treatment with extracellular vesicles using TRIzol reagent (Invitrogen, Carlsbad, CA, USA). RNA was reverse-transcribed using a ReverTra Ace qPCR RT Master Mix (Toyobo Bio-Technology, Osaka, Japan). The following primers were used for sequencing: *TNF-α*, forward: 5'-GA GGC CAA GCC CTG GTA TG-3' and reverse: 5'-CG GGC CGA TTG ATC TCA GC-3'; *COX-2*, forward: 5'-TT GCT GGC AGG GTT GCT GGT-3' and reverse: 5'-TC TGC CTG CTC TGG TCA ATG G-3'; *interleukin 1β (IL-1β)*, forward: 5'-TC CAG GGA CAG GAT ATG GAG-3' and reverse: 5'-CC AAG GCC ACA GGT ATT TTG-3'; *interleukin 6 (IL-6)*, forward: 5'-AA AGA GGC ACT GGC AGA AAA-3' and reverse: 5'-AG CTC TGG CTT GTT CCT CAC-3'; and *GAPDH*, forward: 5-TC GCC CCA CTT GAT TTT GG-3 and reverse: 5-GC AAA TTC CAT GGC ACC GT-3'. The thermal cycling conditions comprised an initial denaturation at 95°C for 15 min, followed by 33 cycles of 94°C for 30 s, 50°C for 30 s, and 72°C for 60 s. Real-

time PCR was performed using the QuantStudio^{TM} 6 Flex Real-Time PCR System (Applied Biosystems, Foster City, CA, USA).

Confocal microscopy

Reactive oxygen species (ROS) were detected using 1 µM 2',7'-dichlorodihydrofluorescein diacetate (DCFDA) in HMEECs. The cells were then incubated in a humidified 5% CO_2 incubator for 30 min at 37°C after treatment with DCFDA. In contrast, CD63, an EV marker, was observed when the MSCs were incubated in 5% normal goat serum for 1 h at RT to prevent non-specific labeling. Anti-CD63 (1:200, ab 118307, Abcam, MA, USA) was used as the primary antibody for 1 h at 4°C. The samples were washed with PBS three times for 5 min each time, followed by incubation with a secondary antibody, goat anti-rabbit IgG H&L (Alexa Fluor 488; 1:1000, ab150077, Abcam, MA, USA), for 1 h at RT. After washing the samples three times for 5 min with PBS, they were immobilized with a mounting solution containing DAPI (4,6-diamidino-2-phenylindole). All the samples were observed by confocal microscopy (Carl Zeiss Microscopy GmbH, Jena, Germany), and the images were analyzed using ZEN lite ver. 2.3.

Nanoparticle Tracking Analysis (NTA)

Extracellular vesicles were quantified based on the MISEV guidelines [21]. The particle concentration, size, and distribution of the isolated MSC-derived EVs were analyzed using a NanoSight NS300 (Malvern Instruments Ltd, Malvern, UK). Typically, 1 mL of a 1:100 diluted MSC-derived EV was prepared for particle visualization and recording of light scattering. Three videos, each of 60 s recordings, were analyzed and plotted to show the EV concentration, size, and distribution.

Transmission electronic microscopy (TEM)

MSCs were fixed in 2.5% glutaraldehyde for 2 h at 4 °C, and the samples were solidified in 2% agar. After washing with 0.1 M cacodylate buffer, the samples were post-fixed in 1% osmium tetroxide (OsO_4). The dehydration steps were performed with 50%–100% ethanol, and the samples were then embedded in Epon resin. The samples were baked overnight in an oven at 65°C, sectioned in an ultramicrotome, and examined by TEM using a field electron emission unit (JEM-1200EX-▯, JEOL).

Western blotting

EVs derived from MSCs were isolated through centrifugation, and the amount of total protein was quantified using the Bradford assay. Protein samples were separated using 10% SDS-PAGE with a mini gel apparatus (Bio-Rad, Hercules, CA, USA) and transferred onto PVDF membranes (T831.1, Merck Millipore, MA, USA). Each membrane was blocked with 3% skim milk in Tris-buffered saline containing 0.05% Tween 20. The primary antibodies anti-CD9 (1:1000, ab92726, Abcam, MA, USA), CD63 (1:1000, ab118307, Abcam, MA, USA), and anti-CD81 (1:1000, ab109201, Abcam, MA, USA) were used as primary antibodies and were incubated overnight at 4°C. Mouse anti-rabbit IgG-HRP (sc-2357, Santa Cruz, CA, USA) was used as a secondary antibody for 1 h. The bands were visualized using enhanced chemiluminescence according to the manufacturer's instructions (Immobilon Crescendo Western HRP substrate, Millipore, Darmstadt, Germany).

The band intensities were quantified using the ChemiDoc XRS+ System (Bio-Rad). All the samples were developed within 10 min to obtain a band.

miRNA analysis

RNA samples prepared from EVs were isolated from the single and co-culture media. The RNA from the EVs was labeled AD-M, BM-M, and T-M derived from single cultured media, such as adipose tissue (AD)-derived MSCs, bone marrow (BM)-derived MSCs, and tonsil (T)-derived MSCs. The RNA from the EVs was labeled as H:AD-M, H:BM-M, and H:T-M derived from co-culture media as AD-MSCs, BM-MSCs, and T-MSCs with HMEECs. The concentration of the sample was confirmed through quality control analysis and was confirmed to be between 0.13 and 0.28 ng/μL. To check the purity and quantity of RNA, a NanoDrop spectrophotometer was used to measure the absorbance at 260 and 280 nm. All raw data were extracted automatically using the Affymetrix data extraction protocol using the Affymetrix GeneChip® Command Console® Software (AGCC). The CEL files were imported, miRNA levels were normalized using the RMA algorithm, the detection above background p-values was calculated for all data, and the results were exported using the Affymetrix® Power Tools (APT) software. Array data were filtered using species-specific annotated probes. Comparative analysis between the test and control samples was performed using fold change. All statistical testing and visualization of differentially expressed genes were conducted using the R statistical language 3.3.3 (https://www.r-project.org/). All the predicted mRNAs from the miRNAs in the EVs were analyzed using the NCBI database, ExoCarta (http://www.exocarta.org/), and Vesiclepedia (http://microvesicles.org/).

Statistical analysis

Statistical analysis was performed using the SPSS statistical package (version 21.0; SPSS Inc., USA). All graphs were plotted using GraphPad PRISM (version 5.0; GraphPad Inc., La Jolla, CA, USA). The descriptive results of continuous variables are expressed as mean ± standard deviation (SD) for normally distributed variables. The means were compared using a two-way analysis of variance. The level of statistical significance was set at $p < 0.05$.

Results

Validation of mesenchymal stem cells derived from adipose tissue, bone marrow, and tonsil using FACS

To confirm the effects of MSCs in various locations in the human body, we obtained MSCs from three different human tissues. Adipose tissue-, bone marrow-, and tonsil-derived MSCs have been reported to have cell proliferation and inflammation alleviation efficacy in various studies [4]. We established conditions for purely separating primary cultured MSCs from fresh tissues, and all the samples were validated with specific markers using FACS (Fig. 1a). All the tissues were collected from human donors at our institute. As shown in Fig. 1b, the expression of CD markers in MSCs was demonstrated as CD90, CD105, and CD73, and CD44 did not show a peak in FACS. The MSCs derived from adipose tissue, bone marrow, and tonsils showed similar morphology using microscopy (Fig. 1c).

They were labeled AD-MSC, BM-MSC, and T-MSC since they are MSCs derived from the adipose tissue, bone marrow, and tonsil, respectively (a) The process of extracting and validating MSCs from three tissues, (b) The validation result of MSCs by FACS. MSCs were positive for CD90, CD105, and CD73 and negative for CD44, (c) Microscopic image of AD-MSC, BM-MSC, and T-MSC (bar=10 μm).

Increased levels of inflammatory markers by LPS on human middle ear epithelial cells

Anti-inflammation research using MSCs has been reported in various fields [4]. In this study, we aimed to compare the anti-inflammatory effect of MSCs derived from three different tissues; therefore, we decided to use an in vitro model that can be used for a clinical study related to inflammation. HMEECs are used in OM research because they are easy to access as an initial model to prove the effect between anti-inflammatory reactions with stem cells [26]. We selected the effective concentration (FC20) that showed 81% from 1 μg/mL viability after 24 h (Fig. 2a) and 83% after 24 h with 1 μg/mL LPS (Fig. 2b) because HMEECs must be maintained to extract cell-derived RNA to measure inflammatory factors. Cell imaging via microscopy showed that dead cells were observed by LPS (Fig. 2c and d). To confirm the expression of inflammatory markers, we designed four primers (*COX-2, TNF-α, IL-1β, and IL-6*) for real-time PCR and found that the expression levels of these markers were increased by 1 μg/mL LPS for 24 h. The expression level increased rapidly after 6 h and remained constant after 24 h (Fig. 2e, f, g, and h).

Evaluated cell viability and ROS reduction in the co-culture condition between HMEEC and MSC derived from adipose tissue, bone marrow, and tonsils

Since it is difficult to directly confirm the anti-inflammatory effect of donor cells using MSCs, we tried to prove the anti-inflammatory effect using EVs generated from the co-culture medium. EVs have been reported to occur even in MSC single cultures [32], but the effect of EVs in the co-culture media has not been reported. We hypothesized that since EVs play a role in cell-cell communication, internal substances (miRNAs, proteins, cytokine etc.) change because of the crosstalk between cells [21, 33]. Therefore, adipose-derived MSCs (AD-MSCs), bone marrow-derived MSCs (BM-MSCs), and tonsil-derived MSCs (T-MSCs) were cultured alone. The EVs in the single culture media were labeled as AD-M, BM-M, and T-M. In addition, AD-, BM-, and T-MSCs were co-cultured with HMEECs in a transwell plate to obtain a co-culture medium. The EVs in the co-culture media between MSCs and HMEECs were labeled H:AD-M, H:BM-M, and H:T-M (Fig. 3a). All the EVs were purified using an exosome isolation kit with high centrifugation and were validated in various ways. The efficacy of the EVs was compared after inducing inflammation with LPS in HMEECs pre-treated with EVs (Fig. 3b).

Cell viability was evaluated, as shown in Fig. 3c. When HMEECs were co-cultured with AD-MSCs, BM-MSCs, and T-MSCs, the cell viability was maintained at over 98% for 3 and 24 h. In other words, it was found that HMEECs and MSCs do not cause toxicity to each other through crosstalk. Interestingly, it was also observed that the ROS levels were reduced by the three MSCs after ROS production was stimulated by LPS in HMEECs (Fig. 3d). This suggests that they can be reduced by substances generated during co-culture with MSCs; therefore, it was hypothesized that the ROS-reducing substances in the co-culture medium were EVs. In addition, the amount of protein was evaluated in EVs through specific EV markers, such as CD9, CD63, and CD81 in co-culture media, and it was observed that the protein expression level gradually increased at 3 and 24 h (Fig. 3e). When co-cultured with AD-MSCs, BM-MSCs, and T-MSCs, the ratio of the amount of protein

showed a similar tendency even when the amount of protein was quantified by area (Fig. 3f). The fluorescence images of EVs were analyzed in MSC culture media using the EV marker CD63 through immunofluorescence (IF) (Fig. 3g). Green fluorescence intensity was detected in the media, except cells, and the phenome of EVs released from the MSC surface was observed through TEM (Fig. 3h). In addition, the EVs dissolved in the media were measured by NTA; the EV size was 87.5 ± 10.1 nm, and the concentration of EV was $5.74 \times 10^{10} \pm 5.88 \times 10^{8}$ particles/mL (Fig. 3i). Therefore, we observed that the three MSCs and HMEECs could be co-cultured without toxicity by crosstalk and that the EVs containing the ROS-reducing material are released in the co-culture media.

Decreased TNF-α, COX-2, IL-1β, and IL-6 in co-culture media

ROS levels were reduced by co-culture with the three MSCs, but we isolated EVs from the media. When the HMEECs were co-cultured with the three MSCs and exposed to LPS, LPS stimulated both the MSCs and HMEECs. To evaluate the efficacy of the purified EVs, they should be isolated from the media and compared with single culture media. The viability of HMEECs was evaluated using EVs isolated from single culture media (AD-M, BM-M, and T-M) and EVs extracted from co-culture media (H:AD-M, H:BM-M, and H:T-M). When LPS was treated at 1 mg/mL for 24 h as EC20, the cell viability was approximately 81%. In contrast, the viability of HMEECs treated with AD-M, BM-M, and T-M for 6–48 h was 98% (Fig. 4a). It also showed that the viability of HMEECs was more than 97% when treated with H:AD-M, H:BM-M, and H:T-M for 6–48 h (Fig. 4b). Since the stability of the extracted EVs was confirmed, we compared the effect of inflammatory factors in HMEECs that induced inflammation by EC20 concentration of LPS.

To evaluate the anti-inflammatory effect of EVs isolated from single and co-culture media, the RNA expression level was confirmed through real-time PCR. To confirm the anti-inflammatory effect of EVs extracted from a single culture medium and co-culture medium, the expression of RNA inflammatory factor generation was observed using real-time PCR. After treating with EVs, the HMEEC cultured media was changed and treated with LPS for 0.5, 1, 3, 6, 24, and 48 h. EVs derived from single culture media, AD-M, BM-M, T-M, showed decreased levels of TNF-α after 1 h of exposure, which were 7.0 ± 0.64 to 4.41 ± 0.17 by AD-M, 3.41 ± 0.13 by BM-M, and 3.34 ± 0.31 by T-M (Fig. 4c). In contrast, EVs derived from the co-culture medium H:AD-M, H:BM-M, and H:TM showed decreased levels of TNF-α after 1 h of exposure, which were 2.53 ± 0.12 by H:AD-M, 0.29 ± 0.04 by H: BM-M, and 2.44 ± 0.04 by H:T-M (Fig. 4c). Interestingly, in the case of EVs derived from co-culture media, the TNF-α expression level did not increase within 1 h by H:BM-M (Fig. 4c). H:AD-M and H:T-M showed similar expression levels to AD-M and T-M. The expression level of COX-2 stimulated by LPS confirmed that BM-M and T-M showed decreased expression levels after 24 h rather than AD-M.

It was also confirmed that the expression of COX-2 was reduced by co-culture medium-derived EVs. EVs derived from single culture media, AD-M, BM-M, and T-M, showed that the expression level of COX-2 decreased after 3 h of exposure, which were 5.59 ± 0.16, 1.71 ± 0.03, 2.83 ± 002, and 1.95 ± 0.01, respectively. In contrast, EVs derived from the co-culture medium H:AD-M, H:BM-M, and H:TM decreased the expression level of COX-2 after 3 h. t was confirmed that the expression level of COX-2 also decreased significantly which showed 1.64 ± 0.08 by H:AD-M, 0.08 ± 0.34 by H: BM-M, and 1.66 ± 0.01 by H:T-M after 1 h (Fig. 4d). In addition, it was confirmed that the IL-1β expression level decreased after 3 h by BM-M and T-M, but not by AD-

M. EVs derived from single culture media, AD-M, BM-M, and T-M, showed that the expression level of IL-1β decreased after 3 h exposure, which were 7.55 ± 0.73 to 3.18 ± 0.02 by AD-M, 4.08 ± 0.04 by BM-M, and 3.64 ± 0.01 by T-M (Fig. 4e). In contrast, EVs derived from the co-culture media H:AD-M, H:BM-M, and H:TM decreased the expression level of IL-1β after 3 h, which were 2.89 ± 0.75 by H:AD-M, 0.35 ± 0.611 by H: BM-M, and 3.44 ± 0.13 by H:T-M. As a result, by EVs derived from the co-culture medium, IL-1β decreased after 1 h, and in particular, H:BM-M significantly reduced the expression of IL-1b after 3 h (Fig. 4e). The expression level of IL-6 was also reduced by EVs derived from MSC culture media after stimulation by LPS. EVs derived from single culture media, AD-M, BM-M, and T-M, showed that the expression level of IL-6 decreased after 3 h exposure, which were 3.43 ± 0.18 to 1.7 ± 0.04 by AD-M, 2.88 ± 0.04 by BM-M, and 2.13 ± 0.02 by T-M (Fig. 4f). In contrast, EVs derived from the co-culture media H:AD-M, H:BM-M, and H:TM decreased the expression level of IL-6 after 3 h, which were 1.33 ± 0.42 by H:AD-M, 0.049 ± 0.15 by H: BM-M, and 1.33 ± 0.64 by H:T-M. Almost all expression levels decreased in the positive control, the AD-M, BM-M, and T-M groups showed no decrease in gene expression levels after 48 h. However, IL-6 was significantly decreased after 30 min by H:BM-M, and the expression level decreased after 3 h (Fig. 4f).

Increased miRNA expression level in EVs by co-culture condition

The inflammatory factors were confirmed to significantly decrease in a short time in H:BM-M; therefore, we hypothesized that it would have been reduced by the factor possessed by EVs. In particular, in H:BM-M, it was hypothesized that the payload of a specific factor increases, and some studies have reported that some of the miRNA levels may vary depending on the co-culture conditions [9, 33, 34].

As a result of miRNA analysis by EVs derived from cultured media in six different environments, we confirmed that a total of 161 miRNA expression levels changed (Fig. 5a). Interestingly, as shown in the heatmap, it was confirmed that the miRNA level increased significantly under co-culture conditions. The miRNA expression level was compared by a fold change value of 1.5 and 2 times (Fig. 5b). At 1.5 times, the expression of miRNA in AD-M and H:AD-M showed an increase of 85 miRNAs and a decrease of 46 miRNAs. The expression level of miRNA in BM-M and H:BM-M showed an increase of 125 miRNAs and a decrease of 5 miRNAs. The expression levels of miRNAs in T-M and H:T-M showed an increase of 126 miRNAs and a decrease of 1 miRNA. In addition, the expression level of miRNA was analyzed as a 2-fold change. There were 69 miRNAs and 34 downregulated miRNAs in the AD-M and H:AD-M groups. There were 102 miRNAs and two decreased miRNAs in BM-M and H:BM-M. There were 117 upregulated miRNAs in the T-M and H:T-M groups. Furthermore, to analyze the miRNAs increased by co-culture, we selected the top five miRNAs with a large increase in expression level. Comparing IAD-M and H:AD-M, the highest miRNA expression was hsa-miR-3960, hsa-miR-2115-5p, hsa-miR-320e, hsa-miR-8075, and hsa-miR-6732-5p (Fig. 5c). In addition, in the results of comparing BM-M and H:BM-M, the highest miRNA expression was hsa-miR-638, hsa-miR-5787, hsa-miR-5189-3p, hsa-miR-6732-5p, and hsa-miR-2115- It is 5p (Fig. 5d). Finally, the results of comparing T-M and H:T-M, the highest miRNA expression were hsa-miR-2115-5p, hsa-miR-5787, hsa-miR-6732-5p, hsa-miR-8075, and hsa-miR-320e (Fig. 5e). Interestingly, miRNAs that overlapped with each other were found, and a large amount of miRNA was observed to increase in H:BM-M.

To confirm the intersection of each EV sample from the three different MSCs, we performed a band diagram analysis and found that a total of 51 miRNAs were changed for overlapping factors under the three

conditions (Fig. 6a). In addition, the number of upregulated miRNAs was 42 under the three conditions (Fig. 6b), and the decreased miRNA did not intersect in the TM vs H:TM samples and one was found in AD-M vs. H:AD-M and BM-M vs H:BM-M (Fig. 6c).

The amyloid-based binding proteins combined to decrease inflammatory factors in H:BM-M

Following the results of miRNA analysis, we analyzed gene ontology (GO) to understand the role and biological function of proteins related to these miRNAs. In a previous experiment, we confirmed that when EVs were pre-treated with HMEEC and then induced inflammation with LPS, the result of rapidly reducing the inflammatory factor after 1 h by EVs derived from co-culture media (Fig. 4). It was assumed that there would be information on useful molecules in H:BM-M, which significantly reduced the gene expression of TNF-α, COX-2, IL-1β, and IL-6 in inflammation-induced cells. Therefore, we analyzed the expression of miR-638, which was highly expressed in H:BM-M.
First, most of the proteins expressed for miR-638 included factors that affected the development of intracellular proteins in donor cells. It is also involved in RNA transcription polymerase-related factors and cell-cell signaling. In addition, there was a small expression level related to the factors involved in differentiation (Fig. 7a).

Next, the relevance of the cellular component was analyzed, and an association with a total of 10 organelles was shown. The predicted proteins were mainly related to the intracellular, membrane, and cytoplasm (Fig. 7b). In addition, among them as a result of analyzing molecular function, it was confirmed that the factors related to protein binding significantly increased. In particular, the expression of the amyloid-beta binding protein was found to be the largest (Fig. 7c). It has been reported that amyloid-beta A4 precursor protein-binding family A member 2 (APBA2) is involved in synaptic transport and junction of neurons [35], but they are also involved in improving immunity and cell regeneration [36]. We hypothesized that the anti-inflammatory effect of HMEECs was increased by the expression of miRNA-638 in H:BM-M and APBA2 could be expected to be a candidate connection protein (Fig. 7d). APBA2 also showed an association of 0.989 with STXBP1 and a low association with NRXN1 and STX1A (Fig. 7e). Therefore, we concluded that BM-MSCs significantly increased the expression of APBA2-related proteins in EVs in the medium by exchanging substances with HMEEC, thereby improving the anti-inflammatory effect of HMEECs.

Discussion

Research on the development of therapeutic materials using human MSC-derived EVs has been actively reported in the field of regenerative medicine and anti-inflammatory materials [5, 37, 38]. Representative human stem cells of various origins, such as adipose tissue, bone marrow, umbilical cord, and tonsil, have been reported [5, 14]. Interestingly, some studies have reported that MSCs derived from different tissues have different payloads to communicate with recipient cells as donor cells by using EVs with a determined size of less than 100 nm [5, 14]. However, there has not been a study comparing the components of MSC-derived EVs of different origins to discover therapeutic materials for inflammatory diseases or cancer diseases.

We hypothesized that EVs derived from different origin influence different inflammatory effects on one recipient cell. Here, we would like to propose that two new facts. 1) The anti-inflammatory effects of EVs

derived from MSCs of different origins are indicated by differences in payloads. 2) Crosstalk between cells by co-culture can improve anti-inflammatory effects by altering the payload of EVs. MSCs were extracted from three different origin (Adipose tissue, Bone marrow, and Tonsil), and the change in payload of EVs obtained by co-culture with middle ear epithelial cells (HMEEC) in transwells was analyzed. Adipose tissue (AD)-derived MSCs express mRNAs related to transcription factors, angiogenesis, and adipogenesis [18, 27]. Bone marrow (BM)-derived MSCs are widely known for their regenerative, immune stimulatory, and related factors, such as calcium signaling and cytoskeletal genes [20]. Tonsil (T)-derived MSCs have been reported as cells whose clinical therapeutic efficacy has been confirmed through studies in which the expression of inflammatory cytokines was increased through injection in acute and chronic colitis models [28, 39]. In this study, using a model that causes otitis media (OM), a disease with a high incidence in children, we confirmed the efficacy of MSC-derived EV to reduce inflammatory factors (TNF-α, COX-2, IL-1β, and IL-6). The expression of inflammatory factors, induces immune regulation, mucosal changes, and inflammatory responses, leading to the development of OM [26]. Among these, *TNF-α*, which plays an important role in the induction of an inflammatory cascade, is known to induce OM [39]. *COX-2* is the major enzyme that converts arachidonic acid to prostaglandin H2 to produce inflammatory mediators. The expression level of *COX-2* was upregulated in the middle ear of patients with OM compared to that in healthy subjects [40]. It has been reported that it can damage hearing if the inflammation of HMEECs increases significantly [41]. OM is mainly focused on in clinical research, but this finding of molecules in stem cell-derived EVs can be valuable in development of a new material by reducing the death of middle ear cells and ROS reduction by inflammatory factors [41].

The viability of HMEECs was over 98% during co-culture with AD-MSCs, BM-MSCs, and T-MSCs, as verified by FACS (Fig. 1b), confirming that no toxic substances were generated. The expression levels of inflammatory markers significantly increased after 24 h of exposure to 1 μg/mL LPS, and the cell viability also decreased to less than 80%. We found that apoptosis was induced by exposure to LPS after 24 h (Fig. 2).

To analyze the change in payload in the MSC-derived EVs that we hypothesized, donor MSCs and recipient HMEECs were co-cultured in trans wells. The EVs were separated from the co-culture medium by centrifugation, and it was confirmed that ROS production induced by LPS was decreased by EVs in HMEECs (Fig. 3d). Based on these results, it was proved that the MSC-derived EVs, which are labeled AD-M, BM-M, and T-M in a single culture, contained factors capable of reducing ROS levels. Furthermore, there might be several useful factors expressed in co-culture media because large amounts of CD9, CD63, and CD81 (EV markers) were found after co-culture of 24 h (Fig. 3e and f). In other words, the co-culture conditions showed that EV generation can be increased by the crosstalk between donor and recipient cells, suggesting that the payload can be changed.

It was confirmed that the size of EVs in the single medium and co-culture media was less than 100 nm (Fig. 3h and i), and the levels of inflammatory factors expressed by LPS were decreased by EVs. The EVs derived from MSC single culture media (AD-M, BM-M, and T-M) reduced the mRNA expression levels of *TNF-α, COX-2, IL-1β*, and *IL6* by half (Fig. 4). Interestingly, among the EVs derived from co-culture media (H:AD-M, H:BM-M, and H:T-M), H:BM-M showed the greatest efficiency in reducing inflammatory factor expression until zero by pretreatment with HMEECs for 3 h. Therefore, we hypothesized that some molecules had been delivered to the recipient cells, which is related to reduced expression of inflammatory factors.

The useful factors contained in EVs and some miRNA databases were analyzed by miRNA analysis (Fig. 5). Using miRNA analysis, we found that 161 miRNAs were expressed under the three co-culture conditions, and these were related to the effects of immunity and proliferation on the cells (described in Table 1). miR-3960 was highly expressed in H:AD-M, H:BM-M, and H:T-M. The predicted mRNA levels were analyzed for POU class 3 homeobox 3 (*POU3F3*) [42], protocadherin alpha 2 (*Pcdha2*) [43], ceramide synthase 1 (*CERS1*) [44], early growth response (*EGR*) [45], and macrophage migration inhibitory factor (*MIF*)[46]. miR-5787 was highly expressed in both H:BM-M and H:T-M cells. The predicted mRNA was analyzed for phosphofurin acidic cluster sorting protein 1 (*PACS1*) [47], protein phosphatase 1 regulatory subunit 7 (*PPP1R7*) [48], visual system homeobox 2 (*VSX2*) [49], SMAD family member 2, SMAD family member 3 [50], and synaptotagmin 1 (*SYT1*) [51]. In addition, miR-6732-5p, miR-8075, miR-320e, and miR-2115-5p expression decreased in the H:AD-M group and increased in the H:BM-M and H:T-M groups (Fig. 8). Interestingly, miR-638, which significantly reduced *TNF-α, COX-2, IL-1β,* and *IL-6* (Fig. 4) expression, showed increased expression only in H:BM-M. One of the predicted mRNAs analyzed Solute carrier family 25-member 23 (*SLC25A23*) and Adhesion G protein-coupled receptor E5 (*ADGRE5*) was reported to be involved in both adhesion and signaling processes [45]. *SLC25A23* reportedly decreases mitochondrial Ca (2+) uptake and reduces cytosolic Ca (2+) clearance after histamine stimulation [51]. In addition, approximately 100 predicted mRNAs were analyzed, and we tried to select the most related proteins through gene ontology analysis. We hypothesized that miR-638-related protein inhibited the increase in inflammatory factors in HMEECs; therefore, we predicted that it was *APBA2* (Fig. 7c). It is cautious to predict proteins that have organic relationships in cells, but we found that *APBA2* can play a role in binding and transmitting factors related to binding to membranes containing immunity and differentiation [36]. *APBA2* encodes a cell surface receptor and transmembrane precursor protein that is cleaved by secretases to form a number of peptides. In addition, two of these peptides are antimicrobial peptides, which have been shown to have bactericidal and antifungal activities. Mutations in this gene are associated with autosomal dominant Alzheimer's disease and cerebral arterial amyloidosis (cerebral amyloid angiopathy). Several transcriptome variants have been discovered that encode several different isotypes of this gene [52]. As reported for EVs to communicate between cells, a major difference among vesicle subtypes is their origin, while microvesicles and ectosomes bud from the plasma membrane, EV formation begins on early endosomes [6, 7]. After maturation in multivesicular bodies through the invagination of the endosomal membrane and formation of intraluminal vesicles (ILVs), EVs are released by the fusion of ILVs with the plasma membrane [14]. The specific proteins incorporated into ILVs are regulated mainly by the endosomal-sorting complex required for transport (ESCRT), of which there are four: ESCRT-0, I, II, and III. As a result, we discussed that binding proteins, such as *APBA2,* can induce and stimulate the transport of inflammatory factors by connecting the cellular membrane. In a study that reported the activity of *APBA2*, it was reported in patients with age-related macular degeneration (AMD), and autophagy factors were identified by treating ARPE-19 cells with soluble amyloid with an oligomer [53]. Autophagy activated in ARPE-19 cells treated with *APBA2* altered the expression pattern of LC3 by creating a phagocytic compartment and activating p62, thus clarifying the potential ambiguity mechanism of retinal cells. It has been reported that *APBA2* is involved in the MAPK signaling pathway and it alters cell viability, migration, and invasion [52]. However, the relationship between amyloid activity and neuroinflammation has been reported [54]; the role of inflammation in auditory hearing loss relief should be explored in further studies.

MSCs were extracted from three tissues and the changes in miRNA payload in EVs and the anti-inflammatory effect of MSC-derived EVs were analyzed in this study. In particular, to improve the anti-inflammatory effect of epithelial cells that induce inflammation, EVs of epithelial cells and MSC co-culture medium were extracted, and the payload was confirmed to change. Therefore, our study predicts that the change in the payload in EVs expressed by co-culture with stem cells can be used in various disease models. The co-culture of stem cells as donor and recipient cells might prove to be valuable in the field of regenerative medicine and material development.

Declarations

Ethics approval and consent to participate

Not applicable

Consent for publication

Not applicable

Availability of data and materials

Not applicable.

Competing interests

The authors declare that they have no competing interests.

Funding

Not applicable.

Acknowledgments

Author contributions

D.J.P. designed and analyzed the entire study of extracellular vesicles through a co-culture approach between MSCs and HMEECs. J.E.P. and T.H.K analyzed biological method and technical support. Y.J.S provided support for this study. D.J.P. wrote the first draft of manuscript, and all the authors have reviewed the manuscript.

Authors' information

[1] Department of Otorhinolaryngology, Yonsei University Wonju College of Medicine, 20 Ilsan-ro, Wonju, Gangwon-do 26426, South Korea. [2] Research Institute of Hearing Enhancement, Wonju, Gangwon-do, 26426,

South Korea. [3] Department of Surgery, University of California San Diego, 212 Dickinson Street, MC 8236, San Diego, CA 92103, USA. [4] School of Pharmacy and Biomedical Sciences, Curtin University, Bentley, WA 6102, Australia

References

1. Sugino H, Tsumura S, Kunimoto M, Noda M, Chikuie D, Noda C, et al. Influence of pneumococcal conjugate vaccine on acute otitis media with severe middle ear inflammation: A retrospective multicenter study. PLoS One. 2015;10:e0137546. https://doi.org/10.1371/journal.pone.0137546

2. Lighthall JG, Kempton JB, Hausman F, MacArthur CJ, Trune DR. Control of middle ear inflammatory and ion homeostasis genes by transtympanic glucocorticoid and mineralocorticoid treatments. PLoS One. 2015;10:e0119228. https://doi.org/10.1371/journal.pone.0119228

3. Sessa R, Hata A. Role of microRNAs in lung development and pulmonary diseases. Pulm Circ. 2013;3:315-28. https://doi.org/10.4103/2045-8932.114758

4. Gowen A, Shahjin F, Chand S, Odegaard KE, Yelamanchili SV. Mesenchymal stem cell-derived extracellular vesicles: challenges in clinical applications. Front Cell Dev Biol. 2020;8:149. https://doi.org/10.3389/fcell.2020.00149

5. Joo HS, Suh JH, Lee HJ, Bang ES, Lee JM. Current knowledge and future perspectives on mesenchymal stem cell-derived exosomes as a new therapeutic agent. Int J Mol Sci. 2020;21. https://doi.org/10.3390/ijms21030727

6. Xiao YW, Zhong JN, Zhong BY, Huang JY, Jiang LX, Jiang Y, et al. Exosomes as potential sources of biomarkers in colorectal cancer. Cancer Lett. 2020;476:13-22. https://doi.org/10.1016/j.canlet.2020.01.033

7. Jeppesen DK, Fenix AM, Franklin JL, Higginbotham JN, Zhang Q, Zimmerman LJ, et al. Reassessment of exosome composition. Cell. 2019;177:428-45 e18. https://doi.org/10.1016/j.cell.2019.02.029

8. Shenoy GN, Bhatta M, Loyall JL, Kelleher RJ, Jr., Bernstein JM, Bankert RB. Exosomes represent an immune suppressive T cell checkpoint in human chronic inflammatory microenvironments. Immunol Invest. 2020;49:726-43. https://doi.org/10.1080/08820139.2020.1748047

9. Chiba M, Kimura M, Asari S. Exosomes secreted from human colorectal cancer cell lines contain mRNAs, microRNAs and natural antisense RNAs, that can transfer into the human hepatoma HepG2 and lung cancer A549 cell lines. Oncol Rep. 2012;28:1551-8. https://doi.org/10.3892/or.2012.1967

10. Preciado S, Muntion S, Sanchez-Guijo F. Improving hematopoietic engraftment: Potential role of mesenchymal stromal cell-derived extracellular vesicles. Stem Cells. 2021;39:26-32. https://doi.org/10.1002/stem.3278

11. Buratta S, Tancini B, Sagini K, Delo F, Chiaradia E, Urbanelli L, et al. Lysosomal exocytosis, exosome release and secretory autophagy: The autophagic- and endo-lysosomal systems go extracellular. Int J Mol Sci. 2020;21:2576. https://doi.org/10.3390/ijms21072576

12. Cheng Q, Li X, Wang Y, Dong M, Zhan FH, Liu J. The ceramide pathway is involved in the survival, apoptosis and exosome functions of human multiple myeloma cells in vitro. Acta Pharmacol Sin. 2018;39:561-8. https://doi.org/10.1038/aps.2017.118

13. Park DJ, Yun WS, Kim WC, Park JE, Lee SH, Ha S, et al. Improvement of stem cell-derived exosome release efficiency by surface-modified nanoparticles. J Nanobiotechnology. 2020;18:178. https://doi.org/10.1186/s12951-020-00739-7

14. Kalluri R, LeBleu VS. The biology, function, and biomedical applications of exosomes. Science (1979). 2020;367:eaau6977. https://doi.org/10.1126/science.aau6977

15. Maas SLN, Breakefield XO, Weaver AM. Extracellular vesicles: unique intercellular delivery vehicles. Trends Cell Biol. 2017;27:172-88. https://doi.org/10.1016/j.tcb.2016.11.003

16. Pisano S, Pierini I, Gu JH, Gazze A, Francis LW, Gonzalez D, et al. Immune (cell) derived exosome mimetics (IDEM) as a treatment for ovarian cancer. Front Cell Dev Biol. 2020;8:553576. https://doi.org/10.3389/fcell.2020.553576

17. Atai NA, Balaj L, van Veen H, Breakefield XO, Jarzyna PA, Van Noorden CJF, et al. Heparin blocks transfer of extracellular vesicles between donor and recipient cells. J Neurooncol. 2013;115:343-51. https://doi.org/10.1007/s11060-013-1235-y

18. Cho BS, Kim JO, Ha DH, Yi YW. Exosomes derived from human adipose tissue-derived mesenchymal stem cells alleviate atopic dermatitis. Stem Cell Res Ther. 2018;9:187. https://doi.org/10.1186/s13287-018-0939-5

19. Lee KE, Jung SA, Joo YH, Song EM, Moon CM, Kim SE, et al. The efficacy of conditioned medium released by tonsil-derived mesenchymal stem cells in a chronic murine colitis model. PLoS One. 2019;14:e0225739. https://doi.org/10.1371/journal.pone.0225739

20. Zhou Y, Zhou W, Chen X, Wang Q, Li C, Chen Q, et al. Bone marrow mesenchymal stem cells-derived exosomes for penetrating and targeted chemotherapy of pancreatic cancer. Acta Pharm Sin B. 2020;10:1563-75. https://doi.org/10.1016/j.apsb.2019.11.013

21. Kulkarni B, Gondaliya P, Kirave P, Rawal R, Jain A, Garg R, et al. Exosome-mediated delivery of miR-30a sensitize cisplatin-resistant variant of oral squamous carcinoma cells via modulating Beclin1 and Bcl2. Oncotarget. 2020;11:1832-45. https://doi.org/10.18632/oncotarget.27557

22. Liang B, Peng P, Chen S, Li L, Zhang M, Cao D, et al. Characterization and proteomic analysis of ovarian cancer-derived exosomes. J Proteomics. 2013;80:171-82. https://doi.org/10.1016/j.jprot.2012.12.029

23. Joshi BS, de Beer MA, Giepmans BG, Zuhorn IS. Endocytosis of extracellular vesicles and release of their cargo from endosomes. ACS Nano. 2020;14:4444-55. https://doi.org/10.1021/acsnano.9b10033

24. Qin S, Dorschner RA, Masini I, Lavoie-Gagne O, Stahl PD, Costantini TW, et al. TBC1D3 regulates the payload and biological activity of extracellular vesicles that mediate tissue repair. FASEB J. 2019;33:6129-39. https://doi.org/10.1096/fj.201802388R

25. Ambattu LA, Ramesan S, Dekiwadia C, Hanssen E, Li H, Yeo LY. High frequency acoustic cell stimulation promotes exosome generation regulated by a calcium-dependent mechanism. Commun Biol. 2020;3:553. https://doi.org/10.1038/s42003-020-01277-6

26. Seo YJ, Choi JY. Expression and localization of aquaporin water channels in human middle ear epithelium. Otol Neurotol. 2015;36:1284-9. https://doi.org/10.1097/MAO.0000000000000797

27. Bacic A, Prgomet D, Janjanin S. Tonsil-derived mesenchymal stem cells exert immunosuppressive effects on T cells. Croat Med J. 2019;60:12-9. https://doi.org/10.3325/cmj.2019.60.12

28. Dominici M, Le Blanc K, Mueller I, Slaper-Cortenbach I, Marini F, Krause D, et al. Minimal criteria for defining multipotent mesenchymal stromal cells. The International Society for Cellular Therapy position statement. Cytotherapy. 2006;8:315-7. https://doi.org/10.1080/14653240600855905

29. Chun YM, Moon SK, Lee HY, Webster P, Brackmann DE, Rhim JS, et al. Immortalization of normal adult human middle ear epithelial cells using a retrovirus containing the E6/E7 genes of human papillomavirus type 16. Annals of Otology Rhinology and Laryngology. 2002;111:507-17. https://doi.org/10.1177/000348940211100606

30. Thery C, Witwer KW, Aikawa E, Alcaraz MJ, Anderson JD, Andriantsitohaina R, et al. Minimal information for studies of extracellular vesicles 2018 (MISEV2018): a position statement of the International Society for Extracellular Vesicles and update of the MISEV2014 guidelines. J Extracell Vesicles. 2018;7:1535750. https://doi.org/10.1080/20013078.2018.1535750

31. Lu K, Li HY, Yang K, Wu JL, Cai XW, Zhou Y, et al. Exosomes as potential alternatives to stem cell therapy for intervertebral disc degeneration: in-vitro study on exosomes in interaction of nucleus pulposus cells and bone marrow mesenchymal stem cells. Stem Cell Res Ther. 2017;8:108. https://doi.org/10.1186/s13287-017-0563-9

32. Bruno S, Porta S, Bussolati B. Extracellular vesicles in renal tissue damage and regeneration. Eur J Pharmacol. 2016;790:83-91. https://doi.org/10.1016/j.ejphar.2016.06.058

33. Danzer KM, Kranich LR, Ruf WP, Cagsal-Getkin O, Winslow AR, Zhu L, et al. Exosomal cell-to-cell transmission of alpha synuclein oligomers. Mol Neurodegener. 2012;7:42. https://doi.org/10.1186/1750-1326-7-42

34. Shimasaki T, Yamamoto S, Arisawa T. Exosome research and co-culture study. Biol Pharm Bull. 2018;41:1311-21. https://doi.org/10.1248/bpb.b18-00223

35. Lee JH, Lau KF, Perkinton MS, Standen CL, Shemilt SJ, Mercken L, et al. The neuronal adaptor protein X11alpha reduces Abeta levels in the brains of Alzheimer's APPswe Tg2576 transgenic mice. J Biol Chem. 2003;278:47025-9. https://doi.org/10.1074/jbc.M300503200

36. Becot A, Volgers C, van Niel G. Transmissible endosomal intoxication: A balance between exosomes and lysosomes at the basis of intercellular amyloid propagation. Biomedicines. 2020;8:272. https://doi.org/10.3390/biomedicines8080272

37. Borgovan T, Crawford L, Nwizu C, Quesenberry P. Stem cells and extracellular vesicles: biological regulators of physiology and disease. Am J Physiol Cell Physiol. 2019;317:C155-C66. https://doi.org/10.1152/ajpcell.00017.2019

38. Eirin A, Riester SM, Zhu XY, Tang H, Evans JM, O'Brien D, et al. MicroRNA and mRNA cargo of extracellular vesicles from porcine adipose tissue-derived mesenchymal stem cells. Gene. 2014;551:55-64. https://doi.org/10.1016/j.gene.2014.08.041

39. Ting PJ, Lin CH, Huang FL, Lin MC, Hwang KP, Huang YC, et al. Epidemiology of acute otitis media among young children: A multiple database study in Taiwan. Journal of Microbiology Immunology and Infection. 2012;45:453-8. https://doi.org/10.1016/j.jmii.2012.06.007

40. Kakiuchi M, Tsujigiwa H, Orita Y, Nagatsuka H, Yoshinobu J, Kariya S, et al. Cyclooxygenase 2 expression in otitis media with effusion. Am J Otolaryngol. 2006;27:81-5.

https://doi.org/10.1016/j.amjoto.2005.07.009

41. Pichichero ME. Helping children with hearing loss from otitis media with effusion. Lancet. 2018;392:533-4. https://doi.org/10.1016/S0140-6736(18)31862-2

42. Yang J, Meng X, Yu Y, Pan L, Zheng Q, Lin W. LncRNA POU3F3 promotes proliferation and inhibits apoptosis of cancer cells in triple-negative breast cancer by inactivating caspase 9. Biosci Biotechnol Biochem. 2019;83:1117-23. https://doi.org/10.1111/cpr.12966

43. Carayon K, Chaoui K, Ronzier E, Lazar I, Bertrand-Michel J, Roques V, et al. Proteolipidic composition of exosomes changes during reticulocyte maturation. J Biol Chem. 2011;286:34426-39. https://doi.org/10.1074/jbc.M111.257444

44. Fan XL, Zhang Y, Li X, Fu QL. Mechanisms underlying the protective effects of mesenchymal stem cell-based therapy. Cell Mol Life Sci. 2020;77:2771-94. https://doi.org/10.1007/s00018-020-03454-6

45. Pio R, Jia ZY, Baron VT, Mercola D, UCI NCI SPECS Consortium Strategic. Early growth response 3 (Egr3) is highly over-expressed in non-relapsing prostate cancer but not in relapsing prostate cancer. PLoS One. 2013;8:e54096. https://doi.org/10.1371/journal.pone.0054096

46. Buschow SI, van Balkom BW, Aalberts M, Heck AJ, Wauben M, Stoorvogel W. MHC class II-associated proteins in B-cell exosomes and potential functional implications for exosome biogenesis. Immunol Cell Biol. 2010;88:851-6. https://doi.org/10.1038/icb.2010.64

47. Valadi H, Ekstrom K, Bossios A, Sjostrand M, Lee JJ, Lotvall JO. Exosome-mediated transfer of mRNAs and microRNAs is a novel mechanism of genetic exchange between cells. Nat Cell Biol. 2007;9:654-U72. https://doi.org/10.1038/ncb1596

48. Gonzales PA, Pisitkun T, Hoffert JD, Tchapyjnikov D, Star RA, Kleta R, et al. Large-scale proteomics and phosphoproteomics of urinary exosomes. J Am Soc Nephrol. 2009;20:363-79. https://doi.org/10.1681/ASN.2008040406

49. Moon PG, Lee JE, You S, Kim TK, Cho JH, Kim IS, et al. Proteomic analysis of urinary exosomes from patients of early IgA nephropathy and thin basement membrane nephropathy. Proteomics. 2011;11:2459-75. https://doi.org/10.1002/pmic.201000443

50. He M, Qin H, Poon TC, Sze SC, Ding X, Co NN, et al. Hepatocellular carcinoma-derived exosomes promote motility of immortalized hepatocyte through transfer of oncogenic proteins and RNAs. Carcinogenesis. 2015;36:1008-18. https://doi.org/10.1093/carcin/bgv081

51. Coppola T, Magnin-Luthi S, Perret-Menoud V, Gattesco S, Schiavo G, Regazzi R. Direct interaction of the Rab3 effector RIM with Ca2+ channels, SNAP-25, and synaptotagmin. J Biol Chem. 2001;276:32756-62. https://doi.org/10.1074/jbc.M100929200

52. Xu J, Ying Y, Xiong G, Lai L, Wang Q, Yang Y. Amyloid beta precursor protein silencing attenuates epithelialmesenchymal transition of nasopharyngeal carcinoma cells via inhibition of the MAPK pathway. Mol Med Rep. 2019;20:409-16. https://doi.org/10.3892/mmr.2019.10293

53. Feng L, Liao X, Zhang Y, Wang F. Protective effects on age-related macular degeneration by activated autophagy induced by amyloid-beta in retinal pigment epithelial cells. Discov Med. 2019;27:153-60.

54. Ismail R, Parbo P, Madsen LS, Hansen AK, Hansen KV, Schaldemose JL, et al. The relationships between neuroinflammation, beta-amyloid and tau deposition in Alzheimer's disease: a longitudinal PET study. J

Neuroinflammation. 2020;17:151. https://doi.org/10.1186/s12974-020-01820-6

55. Kowal J, Arras G, Colombo M, Jouve M, Morath JP, Primdal-Bengtson B, et al. Proteomic comparison defines novel markers to characterize heterogeneous populations of extracellular vesicle subtypes. Proc Natl Acad Sci USA. 2016;113:E968-77. https://doi.org/10.1073/pnas.1521230113

56. Schiavinato A, Becker AK, Zanetti M, Corallo D, Milanetto M, Bizzotto D, et al. EMILIN-3, peculiar member of elastin microfibril interface-located protein (EMILIN) family, has distinct expression pattern, forms oligomeric assemblies, and serves as transforming growth factor beta (TGF-beta) antagonist. J Biol Chem. 2012;287:11498-515. https://doi.org/10.1074/jbc.M111.303578

57. van Herwijnen MJ, Zonneveld MI, Goerdayal S, Nolte-'t Hoen EN, Garssen J, Stahl B, et al. Comprehensive proteomic analysis of human milk-derived extracellular vesicles unveils a novel functional proteome distinct from other milk components. Mol Cell Proteomics. 2016;15:3412-23. https://doi.org/10.1074/mcp.M116.060426

58. Lai RC, Tan SS, Teh BJ, Sze SK, Arslan F, de Kleijn DP, et al. Proteolytic potential of the MSC exosome proteome: Implications for an exosome-mediated delivery of therapeutic proteasome. Int J Proteomics. 2012;2012:971907. https://doi.org/10.1155/2012/971907

59. O'Connor BP, Eun SY, Ye Z, Zozulya AL, Lich JD, Moore CB, et al. Semaphorin 6D regulates the late phase of CD4+ T cell primary immune responses. Proc Natl Acad Sci USA. 2008;105:13015-20. https://doi.org/10.1073/pnas.0803386105

60. Gadola SD, Zaccai NR, Harlos K, Shepherd D, Castro-Palomino JC, Ritter G, et al. Structure of human CD1b with bound ligands at 2.3 angstrom, a maze for alkyl chains. Nat Immunol. 2002;3:721-6. https://doi.org/10.1038/ni821

61. Skogberg G, Gudmundsdottir J, van der Post S, Sandstrom K, Bruhn S, Benson M, et al. Characterization of human thymic exosomes. PLoS One. 2013;8:e67554. https://doi.org/10.1371/journal.pone.0067554

62. Harris EA, Stephens KK, Winuthayanon W. Extracellular vesicles and the oviduct function. Int J Mol Sci. 2020;21:8280. https://doi.org/10.3390/ijms21218280

63. Vats S, Manjithaya R. A reversible autophagy inhibitor blocks autophagosome-lysosome fusion by preventing Stx17 loading onto autophagosomes. Mol Biol Cell. 2019;30:2283-95. https://doi.org/10.1091/mbc.E18-08-0482

64. Stefanini AC, da Cunha BR, Henrique T, Tajara EH. Involvement of kallikrein-related peptidases in normal and pathologic processes. Dis Markers. 2015;2015:946572. https://doi.org/10.1155/2015/946572

65. Yoder JH, Han M. Cytoplasmic dynein light intermediate chain is required for discrete aspects of mitosis in Caenorhabditis elegans. Mol Biol Cell. 2001;12:2921-33. https://doi.org/10.1091/mbc.12.10.2921

66. Jansen RS, Mahakena S, de Haas M, Borst P, van de Wetering K. ATP-binding cassette subfamily C member 5 (ABCC5) functions as an efflux transporter of glutamate conjugates and analogs. J Biol Chem. 2015;290:30429-40. https://doi.org/10.1074/jbc.M115.692103

67. Rismanchi N, Soderblom C, Stadler J, Zhu PP, Blackstone C. Atlastin GTPases are required for Golgi apparatus and ER morphogenesis. Hum Mol Genet. 2008;17:1591-604. https://doi.org/10.1093/hmg/ddn046

68. Miller GW, Ulatowski L, Labut EM, Lebold KM, Manor D, Atkinson J, et al. The α-tocopherol transfer protein is essential for vertebrate embryogenesis. PLoS One. 2012;7:e47402. https://doi.org/10.1371/journal.pone.0047402

69. Verlekar D, Wei SJ, Cho H, Yang S, Kang MH. Ceramide synthase-6 confers resistance to chemotherapy by binding to CD95/Fas in T-cell acute lymphoblastic leukemia. Cell Death Dis. 2018;9:925. https://doi.org/10.1038/s41419-018-0964-4

70. Blanchard N, Lankar D, Faure F, Regnault A, Dumont C, Raposo G, et al. TCR activation of human T cells induces the production of exosomes bearing the TCR/CD3/zeta complex. J Immunol. 2002;168:3235-41. https://doi.org/10.4049/jimmunol.168.7.3235

Tables

Table 1 List of predicted target mRNAs by analysis of miRNAs in EVs derived from the co-culture media (AD-H:AD, BM-H:BM, TM-H:TM)

miRNA	Predicted target mRNA		Function & Detail	Reference	
	Symbol	Full name		ExoCerta, Vesiclepidia	PMID
a) Predicted target genes on the increased expression of miRNA under three conditions (AD-H:AD, BM-H:BM, TM-H:TM)					
miR-3960	POU3F3	POU class 3 homeobox 3	: Regulation of oncogenic signaling pathway : Interaction with SMAD protein and the tumor suppressor PTEN.	VP_5455	[42]
	Pcdha2	Protocadherin alpha 2	: Establishment and function of specific cell-cell connections. : Demonstrate an organization similar to that of B-cell and T-cell receptor gene.	ExoCarta_393086 VP_393086	[43]
	CERS1	Ceramide synthase 1	: Encodes a ceramide synthase enzyme, which catalyzes the synthesis of ceramide : Encodes growth differentiation factor from a monocistronic mRNA.	ExoCarta_10715 VP_10715	[44]
	EGR	Early growth response	: May also play a role in a wide variety of processes including muscle development, lymphocyte development, endothelial cell growth and migration, and neuronal development.	ExoCarta_13654 VP_1959	[45]
	MIF	Macrophage migration inhibitory factor	: Encodes a lymphokine involved in immunoregulation, cell-mediated immunity, and inflammation.	ExoCarta_4282 VP_4282	[46]
b) Predicted target genes on the increased expression of miRNA under two conditions (BM-H:BM, TM-H:TM)					
miR-5787	PACS1	Phosphofurin Acidic Cluster Sorting protein 1	: Plays a role in Nef-mediated downregulation of cell surface MHC-I molecules to the TGN, thereby enabling harmful factors to escape immune surveillance.	ExoCarta_107975 VP_107975	[47]

PPP1R7	Protein Phosphatase 1 Regulatory subunit 7	: Encodes a protein subunit that regulates the activity of the serine/threonine phosphatase, protein phosphatase-1.	ExoCarta_5510 VP_5510	[48]
VSX2	Visual system homeobox 2	: Encodes a homeobox protein originally described as a retina-specific transcription factor.	ExoCarta_338917 VP_338917	[49]
SMAD2, SMAD3	SMAD family member 2, SMAD family member 3	: Functions in the transforming growth factor-beta signaling pathway : Cell proliferation, tumor suppressor.	ExoCarta_4088 VP_4088	[50]
SYT1	Synaptotagmin I	: Ca(2+) sensors in the process of vesicular trafficking and exocytosis.	ExoCarta_6857 VP_6857	[51]

c) Predicted target genes on the increased expression of miRNA on BM-H:BM

miR-638	ADGRE5	Adhesion G protein-coupled receptor E5	: Involved in both adhesion and signaling processes early after leukocyte activation	ExoCarta_976	[46]
	SLC25A23	Solute carrier family 25-member 23	: Decreases mitochondrial Ca (2+) uptake and reduces cytosolic Ca (2+) clearance after histamine stimulation.	ExoCarta_79085 VP_79085	[51]
	Cela3b	Chymotrypsin-like elastase family, member 3B	: Functions in the intestinal transport and metabolism of cholesterol. : Little elastolytic activity.	ExoCarta_67868 VP_67868	[47]
	KDSR	3-ketodihydrosphingosine reductase	: Catalyzes the reduction of 3-ketodihydrosphingosine to dihydrosphingosine.	ExoCarta_2531 VP_2531	[55]
	EMILIN3	Elastin microfibril interfacer 3	: Developing gonads and osteogenic mesenchyme.	ExoCarta_90187 VP_90187	[56]

d) Predicted target genes for miRNa with increased expression on BM-H:BM,TM-H:TM and miRNA with decreased on AD-H:ADM

miR-320e	LAPTM4A	Lysosomal protein transmembrane 4 alpha	: Transport of small molecules across	ExoCarta_9741 VP_9741	[57]

			endosomal and lysosomal membranes.		
	PNRC1	Proline-rich nuclear receptor coactivator 1	: RNA polymerase (pol) II-transcribed genes by functioning as a nuclear receptor coactivator.	ExoCarta_10957 VP_10957	[50]
	SKA3	Spindle and kinetochore associated complex subunit 3	: Component of the spindle and kinetochore-associated protein complex that regulates microtubule attachment to the kinetochores during mitosis.	VP_221150	[46]
	TMEM47	Transmembrane protein 47	: Localized to the ER and the plasma membrane.	ExoCarta_83604 VP_83604	[58]
	SEMA6D	Sema domain, transmembrane domain (TM), and cytoplasmic domain, (semaphorin) 6D	: Secreted and membrane associated proteins. : Axon pathfinding, fasciculation and branching, and target selection.	VP_80031	[59]
miR-8075	TMOD2	Tropomodulin 2	: Actin-capping protein for the slow-growing end of filamentous actin.	ExoCarta_29767 VP_29767	[22]
	ADCY1	Adenylate cyclase 1	: Adenylate cyclase gene family that is primarily expressed in the brain. : Ca(2+)/calmodulin concentration.	ExoCarta_107 VP_107	[48]
	CD1B	CD1b molecule	: Primarily lipid and glycolipid antigens of self or microbial origin to T cells.	ExoCarta_910 VP_910	[60, 61]
	OLFM1	Olfactomedin 1	: Neurogenesis, neural crest formation, dorsal ventral patterning, cell-cell adhesion. : Cell cycle regulation, tumorigenesis, and signaling pathways (Wnt, BMP).	VP_10439	[62, 63]
	PRTG	Protogenin	: Development of various tissues, especially neurogenesis.	VP_283659	[46]
miR-	OAS2	2'-5'-oligoadenylate	: innate immune	ExoCarta_4939	[61]

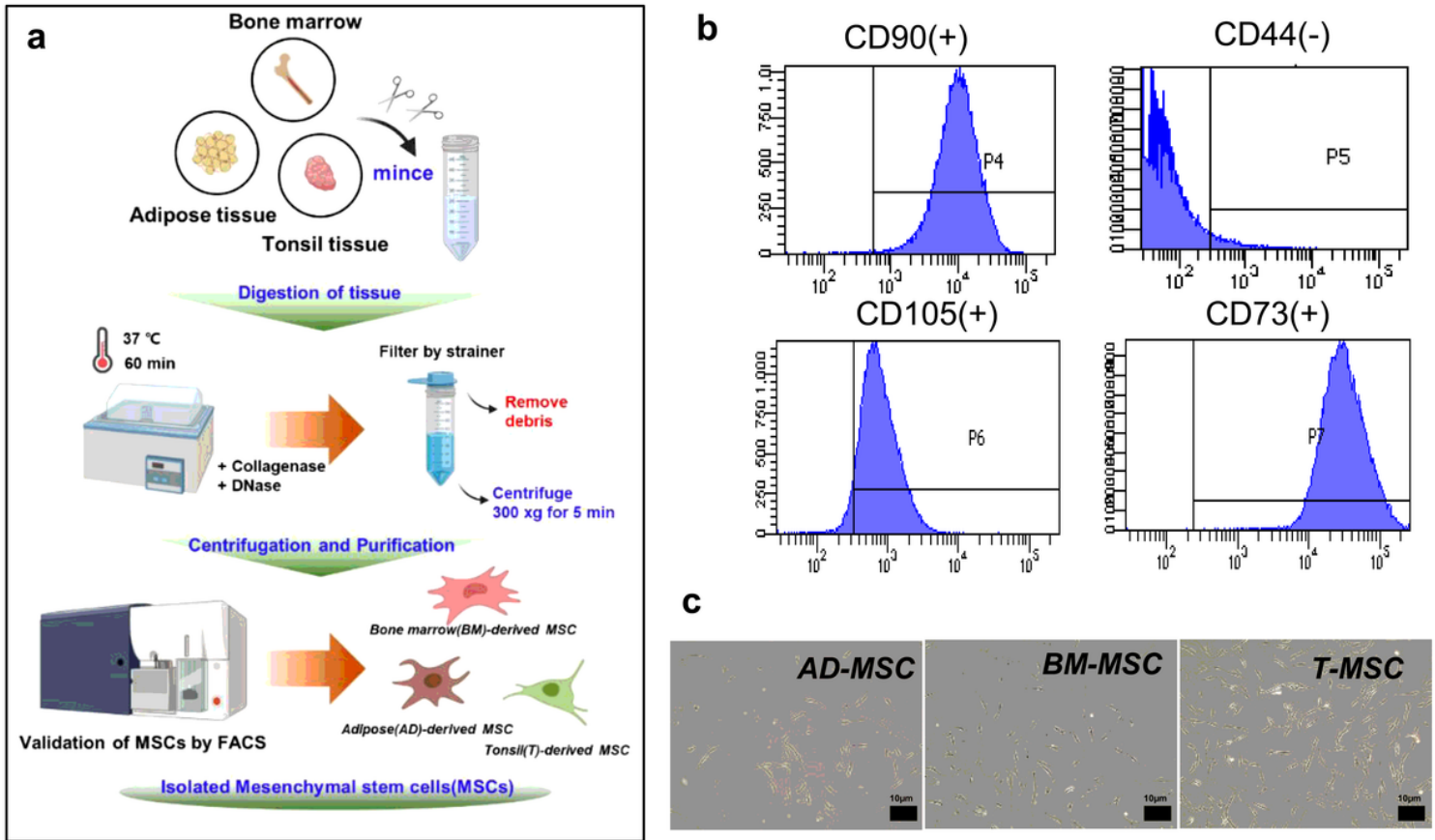|				
6732-5p		synthetase 2, 69/71kDa	response to viral infection	VP_4939	
	STX17	Syntaxin-17	: control of autophagosome membrane fusion with the lysosome membrane		[63]
	KLK3	Kallikrein related peptidase 3	: GPCR signaling pathways, translation Non-genomic (rapid) action of androgen receptor.	VP_354	[64]
	DYNC1LI1	Dynein, cytoplasmic 1, light intermediate chain 1	: Intracellular vesicle trafficking	ExoCarta_51143	[65]
	ABCC5	ATP-binding cassette, sub-family C (CFTR/MRP), member 5	: Resistance to thiopurine anticancer drugs, 6-mercaptopurine and thioguanine functions	ExoCarta_10057 VP_10057	[66]
miR-2115-5p	ATL3	Atlastin GTPase 3	: Network of interconnected tubules of the endoplasmic reticulum	ExoCarta_25923 VP_25923	[67]
	USP49	Ubiquitin specific peptidase 49	: Epigenetic transcriptional activation and acts as a regulator of mRNA splicing.	ExoCarta_25862 VP-25862	[46]
	TTPAL	Alpha tocopherol transfer protein like	: Stimulates the movement of vitamin E between membrane vesicles in vitro and facilitates the secretion of tocopherol from hepatocytes.	N/D (Not detected)	[68]
	CERS6	Ceramide synthase 6	: Cell proliferation, differentiation, apoptosis, and senescence.	ExoCarta_253782 VP_253782	[69]
	CD247	CD247 molecule	: Encodes an immune inhibitory receptor ligand that is expressed by hematopoietic and non-hematopoietic cells, such as T cells and B cells, and various types of tumor cells.	ExoCarta_919 VP_919	[70]

Figures

Figure 1

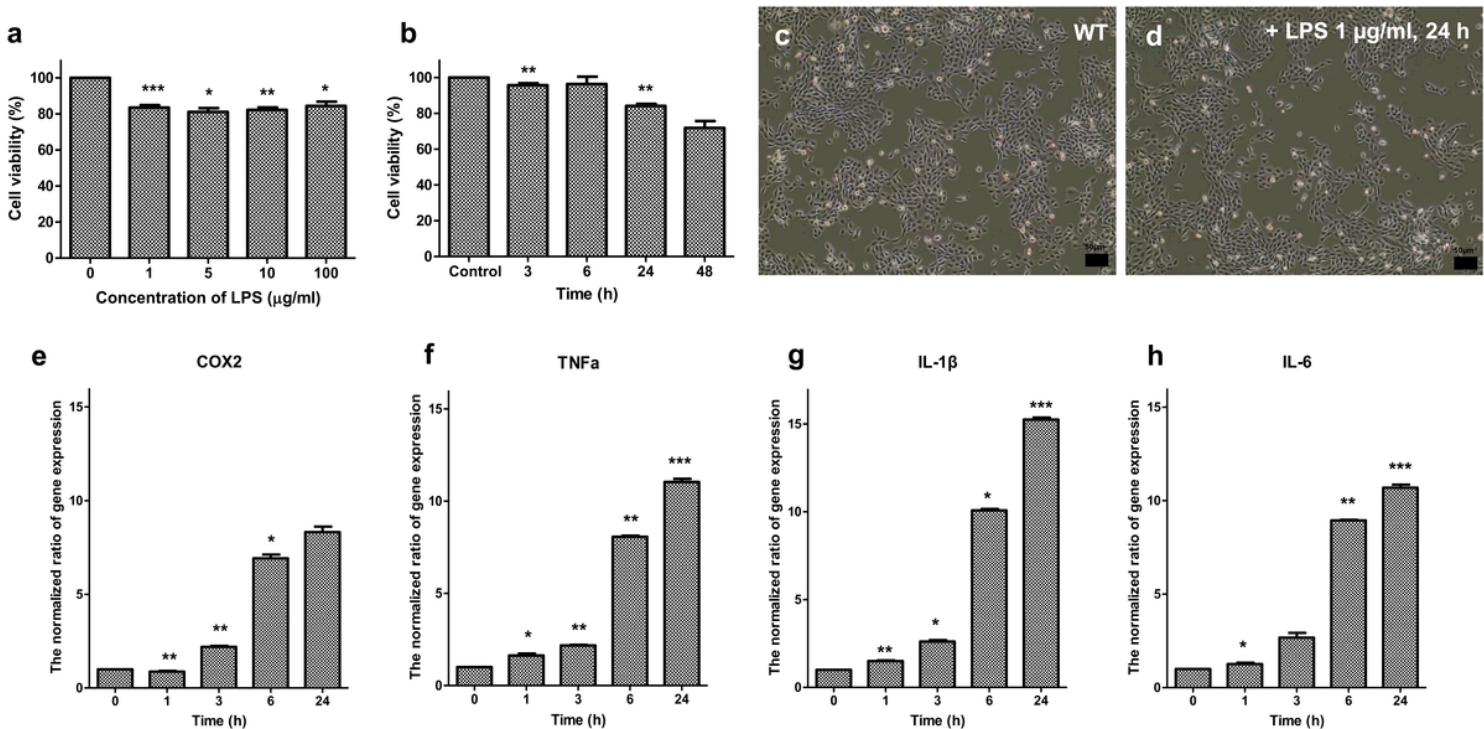Extracted and validated MSCs from the adipose tissue, bone marrow, and tonsil tissue in humans.

Figure 2

Cell viability and expression of TNF-α, COX-2, IL-1β, and IL-6 in HMEECs upon LPS treatment. a The viability of HMEECs after treatment with 1, 5, 10, and 100 μg/mL LPS for 24 h, b The viability of HMEECs treated with 1 μg/mL LPS for 1, 3, 6, 24, and 48 h, c Image of wild-type HMEECs; d Image of HMEECs after treatment with 1 μg/mL LPS for 24 h, e COX-2 expression level in HMEECs after treatment with 1 μg/mL LPS for 24 h, f TNF-α expression level in HMEECs after treatment with 1 μg/mL LPS for 24 h, g IL-1β expression level in HMEECs after treatment with 1 μg/mL LPS for 24 h, h IL-6 expression level in HMEECs after treatment with 1 μg/mL LPS for 24 h (p-value:***<0.001, **<0.01, *<0.05).
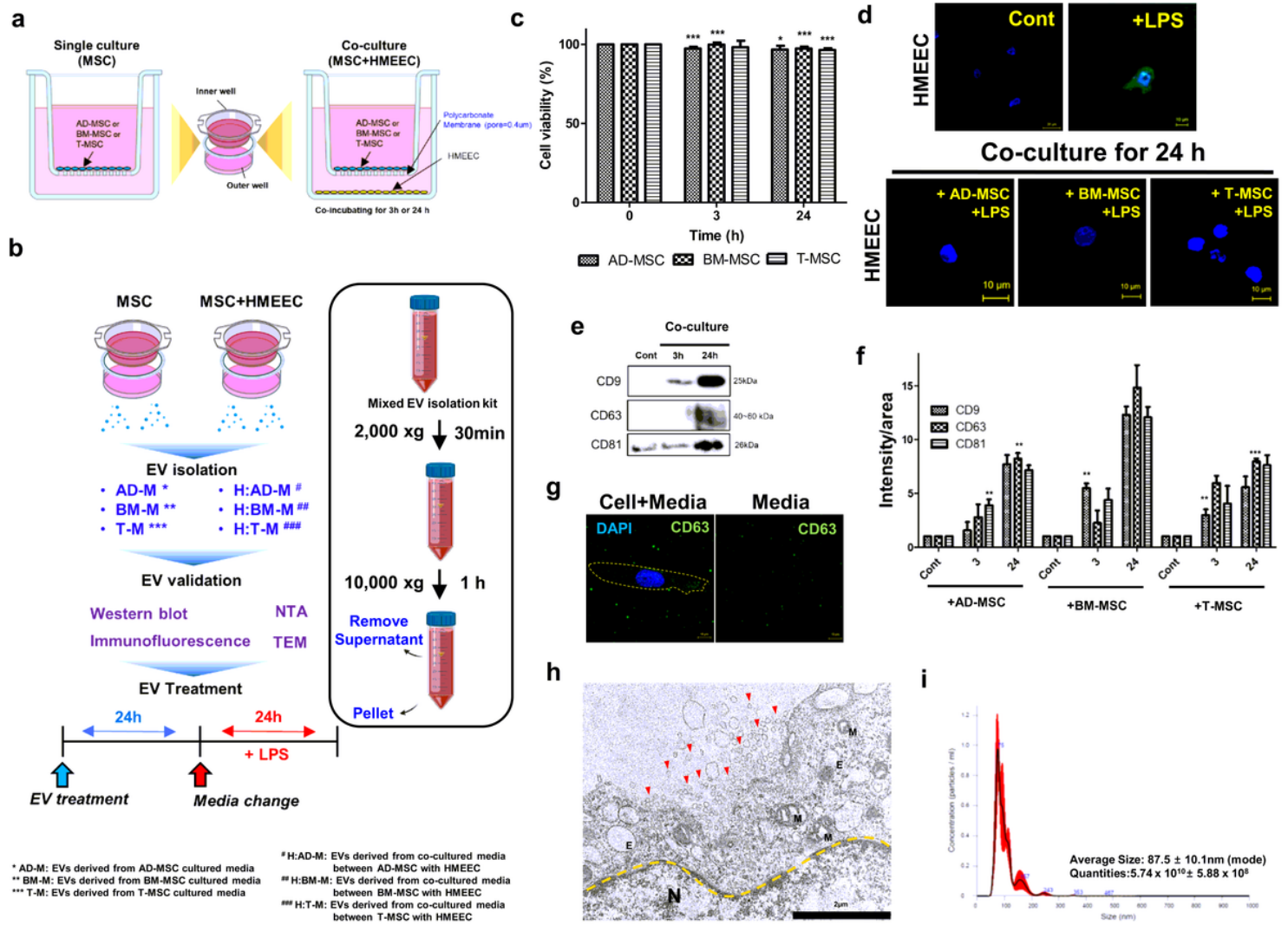

Figure 3

Schematic diagram of co-culture conditions and extraction and evaluation of MSC-derived EVs. a Scheme of culture condition, b Flow chart for EV isolation and treatment of HMEECs, c The viability of HMEECs when co-cultured with AD-MSC, BM-MSC, and T-MSC for 3 and 24 h (p-value:***<0.001, **<0.005, *<0.05), d Evaluation of ROS reduction in HMEECs treated with LPS after co-culture with AD-MSC, BM-MSC, and T-MSC for 24 h, e The expression of CD9, CD63, and CD81 protein bands in the co-culture media, f The normalized intensity of CD9, CD63, and CD81 with the area in the co-culture media (p-value:***<0.001, **<0.005, *<0.05), g The expression of CD63 as an EV marker in the MSC culture media (yellow circle represents the cellular

membrane), h The image of EVs (red arrow) released from the MSC, i The size and concentration analysis in EVs by NTA.
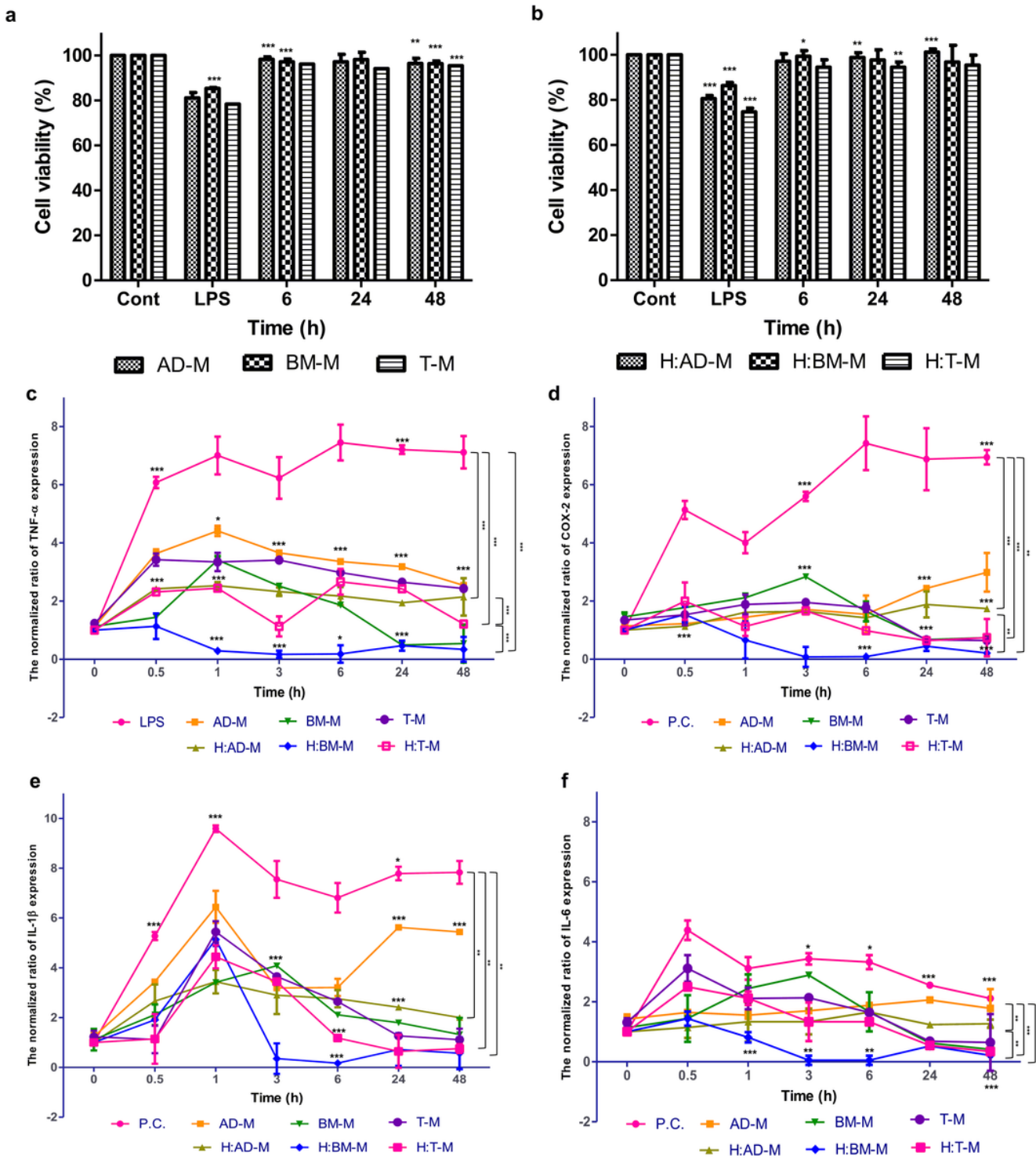

Figure 4

Evaluation of inflammatory markers (TNF-α, COX-2, IL-1β, and IL-6) using EVs derived from the three different co-culture media. a The viability of HMEECs at 6, 24, and 48 h after treatment with EVs (AD-M, BM-M, and T-M) derived from single culture media, b The viability of HMEECs at 6, 24, and 48 h after treatment with EVs (H:AD-M, H:BM-M, and H:T-M) derived from co-culture media, c TNF-α expression level in HMEECs after

treatment with six EVs with 1 µg/mL LPS until 48 h (p-value:***<0.0001), d COX-2 expression level in HMEECs after treatment with six EVs with 1 µg/mL LPS until 48 h (p-value:***<0.0001, **<0.005), e IL-1β expression level in HMEECs after treatment with six EVs with 1 µg/mL LPS until 48 h (p-value: **<0.005), h IL-6 expression level in HMEECs after treatment with six EVs with 1 µg/mL LPS until 48 h (p-value:***<0.001, ** <0.005, *<0.05)
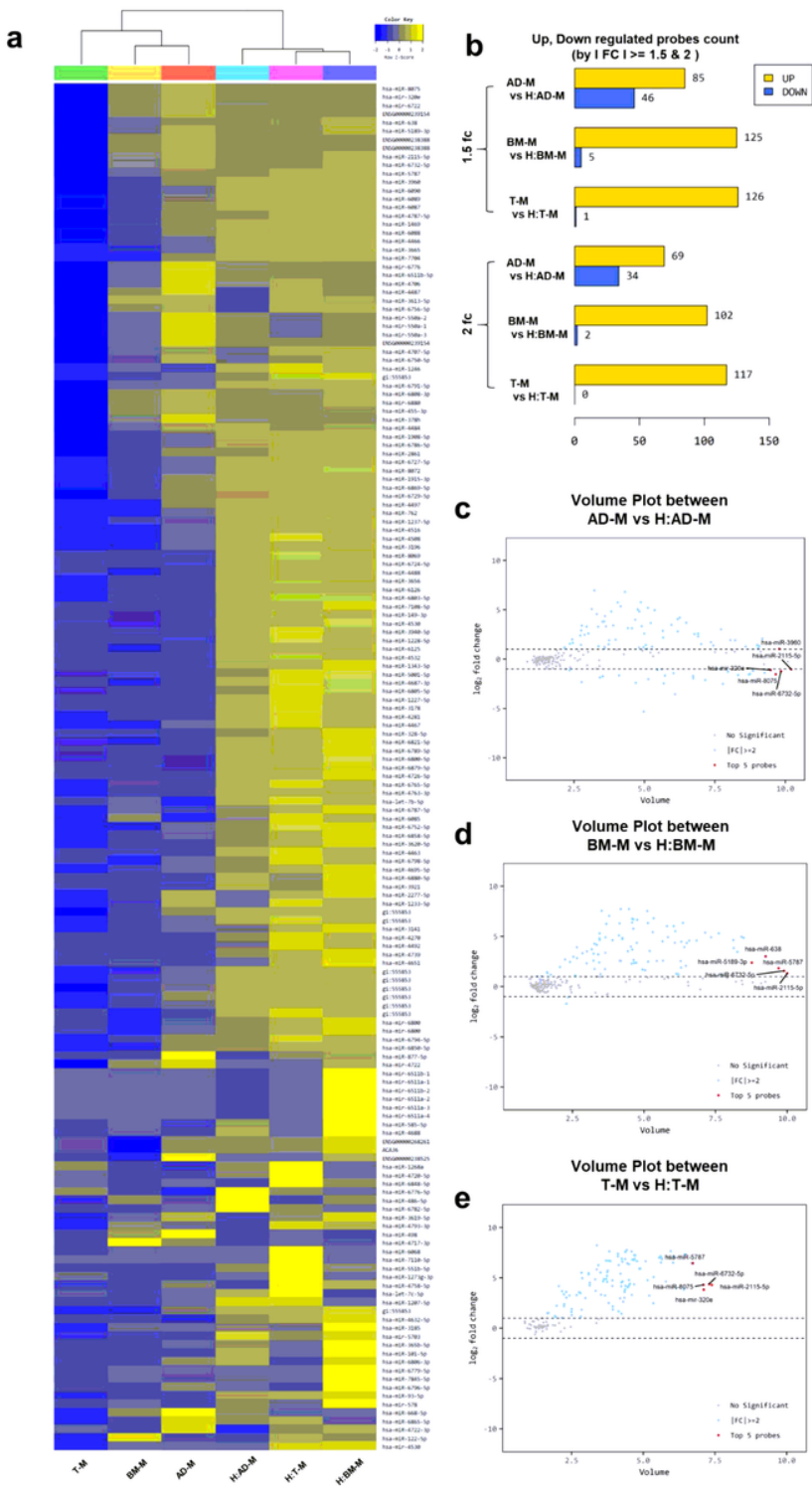

Figure 5

The data of miRNA analysis. a The heatmap of miRNA expression in EVs (AD-M, BM-M, T-M, H:AD-M, H:BM-M, and H:T-M), b The comparison of probe count in up- and downregulation between the six EVs, c The volume plot between AD-M and H:AD-M, d The volume plot between BM-M and H:BM-M, e The volume plot between T-M and H:T-M.
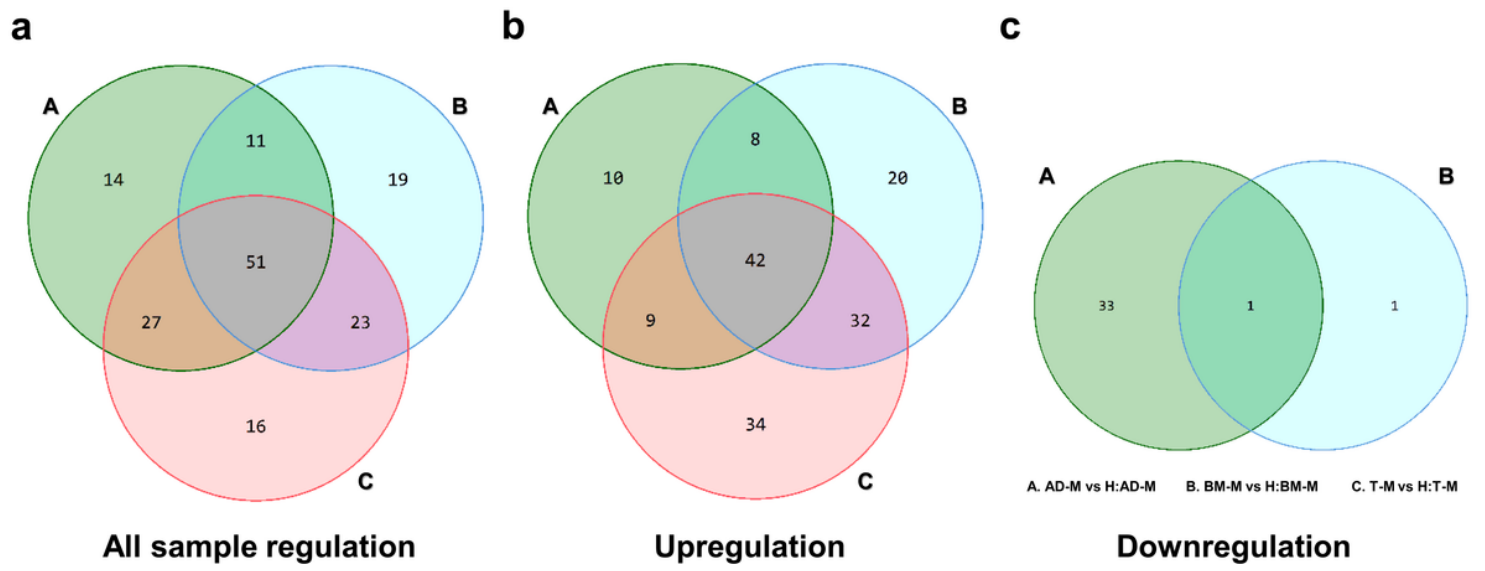

a All sample regulation

b Upregulation

c Downregulation

A. AD-M vs H:AD-M   B. BM-M vs H:BM-M   C. T-M vs H:T-M

Figure 6

Venn diagram of logical miRNA relations in EVs (A, AD-M and H:AD-M; B, BM-M and H:BM-M; c, T-M and H:T-M). a Total regulation of all miRNA regulation for three groups, b Upregulation, c downregulation.
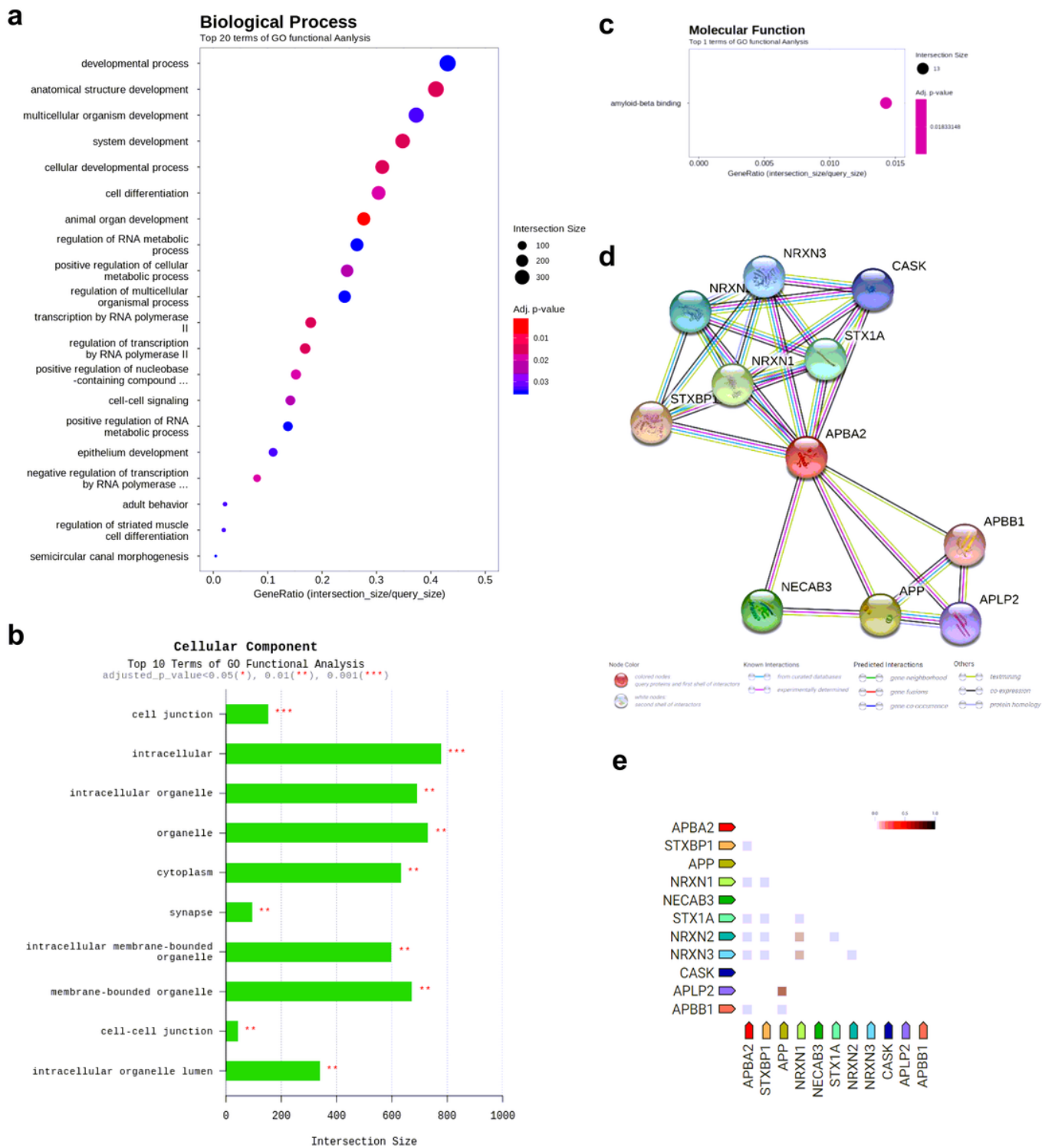
Figure 7

Gene ontology analysis by miRNA in EVs derived from co-culture media between BM-M and H:BM-M. a The analysis of biological process, b The analysis of cellular component, c The analysis of molecular function, d The analysis of protein connection in APBA2, e The comparison analysis of APBA2 with other proteins.